Electromagnetically induced transparency and quadripartite macroscopic entanglement generated in a ring cavity*

Ma Yong-Hong(马永红)[a)b)†] and Zhou Ling(周 玲)[a)‡]

[a)] School of Physics and Optoelectronics Engineering, Dalian University of Technology, Dalian 116024, China
[b)] School of Mathematics, Physics and Biological Engineering, Inner Mongolia University of Science and Technology, Baotou 014010, China

(Received 25 May 2012; revised manuscript received 21 June 2012)

We propose a feasible scheme to generate electromagnetically induced transparency (EIT) and quadripartite macroscopic entanglement in an optomechanical system with one fixed mirror and three movable perfectly reflecting mirrors. We explore the EIT phenomena in this optomechanical system. Results show the appearance of EIT dips in the output field. Moreover, we demonstrate how steady-state quadripartite entanglement can be generated via radiation pressure. We also quantify the bipartite entanglement in each field–mirror subsystem and in the mirror–mirror subsystem. Findings show that a high intensity of entanglement between two subsystems can be achieved.

Keywords: electromagnetically induced transparency, optomechanical system, quadripartite macroscopic entanglement

PACS: 42.50.Dv, 03.67.Mn **DOI:** 10.1088/1674-1056/22/2/024204

1. Introduction

Entanglement, as a characteristic trait of quantum mechanics, has become a key resource for numerous quantum information processing applications.[1] At present, one can experimentally prepare and manipulate entanglement in such microscopic systems as photons, ions, and atoms.[2] However, this advancement will not violate the principle that entanglement can be generated in mesoscopic and even macroscopic systems. Entanglement among macroscopic systems has become a relevant topic since the emergence of quantum mechanics. Therefore, determining the possibility of obtaining quantum entanglement at the macroscopic level is of great importance.

Nanomechanical oscillators are emerging as important candidates for exploring quantum features in a macroscopic system.[3–12] Over the past several years, various schemes for the generation of bipartite entanglement were proposed. The optomechanical entanglement between a cavity field and a vibrating cavity end mirror is investigated in Refs. [13] and [14]. Moreover, a large number of proposals have been put forward on entangling two mirrors in a cavity.[15–18] To date, few authors have investigated multipartite macroscopic entanglement in a mechanical oscillator system. Paternostro *et al.* recently proposed a scheme showing that genuine tripartite entanglement can be achieved via a cavity system using a movable mirror.[19] To the best of our knowledge, no report has been made on quadripartite macroscopic entanglement generation in an optomechanical system.

On the other hand, electromagnetically induced transparency (EIT), as one of the most important coherent effects, has been widely researched both in theory[20–25] and experiments.[26] EIT has significant applications in the storage of light.[27–29] Traditional EIT experiments are based on atomic systems or on a number of systems with coherent pump and probe fields.[30] EIT in cavity optomechanical systems has recently attracted considerable interest.[3,31,32] Notably, EIT in optomechanical systems has been achieved in experiments.[33–35]

In this paper, we propose a scheme to recreate the EIT phenomena and a stationary quadripartite macroscopic entanglement. Our scheme is achieved using a laser field inside a ring cavity and coupled to the position and momentum of three mirrors. We show that EIT dips exist in the output field, and genuine quadripartite macroscopic entanglement can be created in the optomechanical system, although no direct interaction among the three mirrors is observed. The feasible experimental parameters are derived from current experiments on optomechanical normal mode splitting.[36,37] In contrast to previous proposals,[16] temperatures need not be close to the oscillator's ground state. Quadripartite entanglement is shown to exist above a temperature of 9 mK in this case.

2. EIT of a homodyne spectrum

The proposed optomechanical system comprises a ring cavity with one partially fixed transmitting mirror and three movable perfectly reflecting mirrors and is driven by a laser,

*Project supported by the National Natural Science Foundation of China (Grant Nos. 11164018 and 11074028), the Postdoctoral Science Foundation of China (Grant No. 2011M500808), and the Key Project of the Chinese Ministry of Education (Grant No. 212028).

†Corresponding author. E-mail: myh_dlut@126.com
‡Corresponding author. E-mail: zhlhxn@dlut.edu.cn

© 2013 Chinese Physical Society and IOP Publishing Ltd

as shown in Fig. 1.

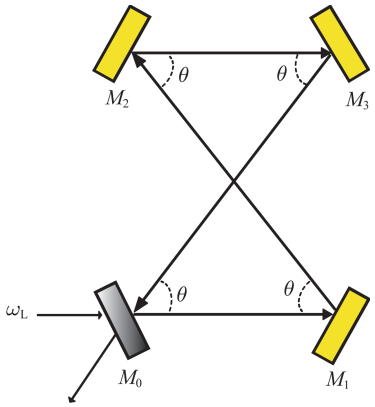


Fig. 1. (color online) A ring cavity with one fixed partially transmitting mirror M_0 and three movable perfectly reflecting mirrors labeled as M_1, M_2, and M_3.

The movable mirrors M_1, M_2, and M_3 are treated as quantum-mechanical oscillators with the same effective masses m and frequencies $\omega_{\rm m}$. An external laser with frequency $\omega_{\rm L}$ is injected into the cavity through the fixed mirror M_0. The Hamiltonian of this system is expressed as

$$\begin{aligned} H &= \hbar(\omega_{\rm c}-\omega_{\rm L})n_{\rm c}+\hbar g n_{\rm c}\cos^2(\theta/2)(Q_2-Q_1-Q_3) \\ &\quad +\frac{1}{2}\hbar\omega_{\rm m}\sum_{i=1,2,3}(Q_i^2+P_i^2)+{\rm i}\hbar\varepsilon(c^\dagger-c), \end{aligned} \tag{1}$$

where Q_j and P_j (j=1, 2, 3) are the position and momentum operators for the oscillators, respectively, with the relationship $[Q_i,P_j]={\rm i}\delta_{ij}$ ($i,j=1,2,3$). g is the coupling rate between the cavity field and the j-th mirror. $c^\dagger$ and c are the creation and annihilation operators of the cavity mode, respectively, with frequency $\omega_{\rm c}$ and decay rate κ. $n_{\rm c}=c^\dagger c$ is the mean photon number inside the ring cavity. θ is the angle between the incident light and the reflected light on the surfaces of the movable mirrors. The parameter ε means the coupling strength between the laser and the cavity with $\varepsilon=\sqrt{2\kappa\zeta/\hbar\omega_{\rm c}}$ (ζ is the power of the coupling field). Using the Heisenberg equations of motion while including the effect of damping and noises, we can obtain the quantum Langevin equations

$$\begin{aligned} \dot{Q}_1 &= \omega_{\rm m}P_1, \\ \dot{Q}_2 &= \omega_{\rm m}P_2, \\ \dot{Q}_3 &= \omega_{\rm m}P_3, \\ \dot{P}_1 &= gn\cos^2(\theta/2)-\omega_{\rm m}Q_1-\gamma_{\rm m}P_1+\xi_1, \\ \dot{P}_2 &= -gn\cos^2(\theta/2)-\omega_{\rm m}Q_2-\gamma_{\rm m}P_2+\xi_2, \\ \dot{P}_3 &= gn\cos^2(\theta/2)-\omega_{\rm m}Q_3-\gamma_{\rm m}P_3+\xi_3, \\ \dot{c} &= -\kappa c+{\rm i}[\omega_{\rm L}-\omega_{\rm c}-g\cos^2(\theta/2)(Q_2-Q_1-Q_3)]c \\ &\quad +\varepsilon+\sqrt{2\kappa}c_{\rm in}, \\ \dot{c}^\dagger &= -\kappa c^\dagger-{\rm i}[\omega_{\rm L}-\omega_{\rm c}-g\cos^2(\theta/2)(Q_2-Q_1-Q_3)]c^\dagger \\ &\quad +\varepsilon+\sqrt{2\kappa}c_{\rm in}^\dagger. \end{aligned} \tag{2}$$

In the proposed system, the movable mirrors are damped at the same damping rate $\gamma_{\rm m}$. Meanwhile, vacuum radiation input noise $X_{\rm in}=c_{\rm in}^\dagger+c_{\rm in}$ and $Y_{\rm in}={\rm i}(c_{\rm in}^\dagger-c_{\rm in})$ is observed, wherein the nonzero correlation function is[38]

$$\langle c_{\rm in}(t)c_{\rm in}^\dagger(t')\rangle=\delta(t-t'). \tag{3}$$

The thermal Langevin force ξ_i (i = 1, 2, 3) results from the coupling of the movable mirror to the environment and is expressed by the following correlation function[39]

$$\begin{aligned} \langle\xi_j(t)\xi_k(t')\rangle &= \frac{\delta_{jk}\gamma_{\rm m}}{2\pi\omega_{\rm m}}\int\omega\,{\rm e}^{-{\rm i}\omega(t-t')} \\ &\quad\times\left[1+\coth\left(\frac{\hbar\omega}{2k_{\rm B}T}\right)\right]{\rm d}\omega, \end{aligned} \tag{4}$$

where $k_{\rm B}$ is the Boltzmann constant and T is the temperature of the environment with $j,k=1,2,3$. Assuming that the relative distance and the relative momentum of the movable mirrors satisfy the relation $Q=Q_2-Q_1-Q_3$, $P=P_2-P_1-P_3$, we reduce Eq. (2) to

$$\begin{aligned} \dot{Q} &= \omega_{\rm m}P, \\ \dot{P} &= -\omega_{\rm m}Q-\gamma_{\rm m}P-3g\cos^2(\theta/2)c^\dagger c+\xi, \\ \dot{c} &= -\kappa c+{\rm i}[\omega_{\rm L}-\omega_{\rm c}-g\cos^2(\theta/2)Q]c \\ &\quad +\varepsilon+\sqrt{2\kappa}c_{\rm in}, \\ \dot{c}^\dagger &= -\kappa c^\dagger-{\rm i}[\omega_{\rm L}-\omega_{\rm c}-g\cos^2(\theta/2)Q]c^\dagger \\ &\quad +\varepsilon+\sqrt{2\kappa}c_{\rm in}^\dagger. \end{aligned} \tag{5}$$

From the above equations, the steady-state mean values can be derived, such as $P^{\rm s}=0$, $Q^{\rm s}=-3g|c^{\rm s}|^2\cos^2(\theta/2)/\omega_{\rm m}$, $c^{\rm s}=\varepsilon/(\kappa+{\rm i}\Delta)$, $\Delta=\omega_{\rm c}-\omega_{\rm L}+g\cos^2(\theta/2)Q^{\rm s}$. To study the EIT in the homodyne spectrum of the output field, we can arrive at the linearized equations for the fluctuation operators

$$\begin{aligned} \delta\dot{Q} &= \omega_{\rm m}\delta P, \\ \delta\dot{P} &= -\omega_{\rm m}\delta Q-\gamma_{\rm m}\delta P-3g\cos^2(\theta/2)[c_{\rm s}\delta c^\dagger+c_{\rm s}^*\delta c]+\xi, \\ \delta\dot{c} &= [-\kappa+{\rm i}(\omega_{\rm L}-\omega_{\rm c}-g\cos^2(\theta/2)Q_{\rm s})]\delta c \\ &\quad -{\rm i}g\cos^2(\theta/2)c_{\rm s}\delta Q+\sqrt{2\kappa}c_{\rm in}, \\ \delta\dot{c}^\dagger &= [-\kappa-{\rm i}(\omega_{\rm L}-\omega_{\rm c}-g\cos^2(\theta/2)Q_{\rm s})]\delta c^\dagger \\ &\quad +{\rm i}g\cos^2(\theta/2)c_{\rm s}^*\delta Q+\sqrt{2\kappa}c_{\rm in}^\dagger. \end{aligned} \tag{6}$$

After Fourier relation, the above equation can be transformed as

$$\begin{aligned} {\rm i}\omega\delta Q(\omega) &= \omega_{\rm m}\delta P(\omega), \\ {\rm i}\omega\delta P(\omega) &= -\omega_{\rm m}\delta Q(\omega)-\gamma_{\rm m}\delta P(\omega)-3g\cos^2(\theta/2) \\ &\quad\times[c_{\rm s}\delta c^\dagger(\omega)+c_{\rm s}^*\delta c(\omega)]+\xi(\omega), \\ {\rm i}\omega\delta c(\omega) &= [-\kappa+{\rm i}(\omega_{\rm L}-\omega_{\rm c}-g\cos^2(\theta/2)Q_{\rm s})]\delta c(\omega) \\ &\quad -{\rm i}g\cos^2(\theta/2)c_{\rm s}\delta Q(\omega)+\sqrt{2\kappa}c_{\rm in}(\omega), \\ {\rm i}\omega\delta c^\dagger(\omega) &= [-\kappa-{\rm i}(\omega_{\rm L}-\omega_{\rm c}-g\cos^2(\theta/2)Q_{\rm s})]\delta c^\dagger(\omega) \\ &\quad +{\rm i}g\cos^2(\theta/2)c_{\rm s}^*\delta Q(\omega)+\sqrt{2\kappa}c_{\rm in}^\dagger(\omega). \end{aligned} \tag{7}$$

in the frequency domain, the operators ξ and $c_{\rm in}$ have the following correlation functions:

$$\begin{aligned}
&\langle \xi_j(\omega)\xi_k(\omega')\rangle \\
&= 4\pi\gamma_{\rm m}\frac{\omega}{\omega_{\rm m}}\left[1+\coth\left(\frac{\hbar\omega}{2k_{\rm B}T}\right)\right]\delta_{jk}\delta(\omega+\omega'), \\
&\langle c_{\rm in}(\omega)c_{\rm in}(\omega')\rangle \\
&= 2\pi\frac{M\Gamma^2}{\Gamma^2+(\omega-\omega_{\rm m})^2}\delta(\omega+\omega'-2\omega_{\rm m}), \\
&\langle c_{\rm in}(\omega)c_{\rm in}^{\dagger}(-\omega')\rangle \\
&= 2\pi\left[\frac{N\Gamma^2}{\Gamma^2+(\omega-\omega_{\rm m})^2}+1\right]\delta(\omega+\omega'), \qquad (8)
\end{aligned}$$

where the parameter N denotes the photon number in the squeezed vacuum with $M=\sqrt{N(N+1)}$, and the parameter Γ is the linewidth of the squeezed vacuum. According to Fig. 2 in Ref. [3], which sketches the measurement of the output field. in our system, we can define the output field as $d_{\rm out}(\omega)=c_{\rm out}(\omega)+c_{\rm in}(\omega)$, and we can derive the result

$$\begin{aligned}
\delta d_{\rm out}(\omega) &= M_1(\omega)\xi(\omega)+M_2(\omega)c_{\rm in}^{\dagger}(-\omega) \\
&\quad + M_3(\omega)c_{\rm in}(\omega), \qquad (9)
\end{aligned}$$

where $M_1=H_1/G$, $M_2=H_2/G$, and $M_3=2\kappa/G$ with

$$\begin{aligned}
G &= D-B-\frac{9g^4\cos^8(\theta/2)|c^{\rm s}|^4}{A(FA+3{\rm i}g^2\cos^4(\theta/2)|c^{\rm s}|^2)}, \\
A &= \frac{(\omega_{\rm m}^2-\omega^2+{\rm i}\gamma_{\rm m}\omega)(F+B)}{\omega_{\rm m}}, \\
B &= \frac{3{\rm i}g^2\cos^4(\theta/2)|c^{\rm s}|^2}{A}, \\
H_1 &= \frac{{\rm i}\sqrt{2\kappa}g\cos^2(\theta/2)c^{\rm s}\omega_{\rm m}(3{\rm i}g^2\cos^4(\theta/2)|c^{\rm s}|^2-F-B_2)}{(\omega_{\rm m}^2-\omega^2+{\rm i}\gamma_{\rm m}\omega)(F+B)}, \\
H_2 &= \frac{6i\kappa g^2\cos^4(\theta/2)|c^{\rm s}|^2}{AG(F+B)},
\end{aligned}$$

$F=\kappa+{\rm i}(\omega-\Delta)$, and $D=\kappa+{\rm i}(\omega+\Delta)$. In Eq. (9), the first term denotes the thermal noise of the three movable mirrors, and the other two terms refer to the contribution of the squeezed vacuum. Using the correlation function of the operators $c_{\rm in}(\omega)$ and $\xi(\omega)$ and neglecting fast oscillating terms, the homodyne spectrum $X(\omega)$ of the output field can be described as

$$\begin{aligned}
X(\omega) &= M_3(\omega+\omega_{\rm m})M_3(-\omega+\omega_{\rm m})\frac{M\Gamma^2}{\Gamma^2+\omega^2} \\
&\quad + |M_3(\omega+\omega_{\rm m})|^2\frac{N\Gamma^2}{\Gamma^2+\omega^2} \\
&\quad + M_3^*(\omega+\omega_{\rm m})M_3^*(-\omega+\omega_{\rm m})\frac{M\Gamma^2}{\Gamma^2+\omega^2} \\
&\quad + |M_3(-\omega+\omega_{\rm m})|^2\frac{N\Gamma^2}{\Gamma^2+\omega^2}+|M_3(\omega+\omega_{\rm m})|^2 \\
&\quad + |M_2(-\omega+\omega_{\rm m})|^2+\gamma_{\rm m}|M_1(\omega+\omega_{\rm m})|^2\frac{\omega+\omega_{\rm m}}{\omega_{\rm m}} \\
&\quad \times\left\{1+\coth\left[\frac{\hbar(\omega+\omega_{\rm m})}{2k_{\rm B}T}\right]\right\}+2\gamma_{\rm m}|M_1(-\omega+\omega_{\rm m})|^2 \\
&\quad \times\frac{\omega+\omega_{\rm m}}{\omega_{\rm m}}\left\{1+\coth\left[\frac{\hbar(\omega-\omega_{\rm m})}{2k_{\rm B}T}\right]\right\}.
\end{aligned}$$

After deriving the above homodyne spectrum equation, we will examine it numerically to study the EIT phenomena in the homodyne spectrum of the output field. The choice of parameters is taken from the experimental paper.[36,37]

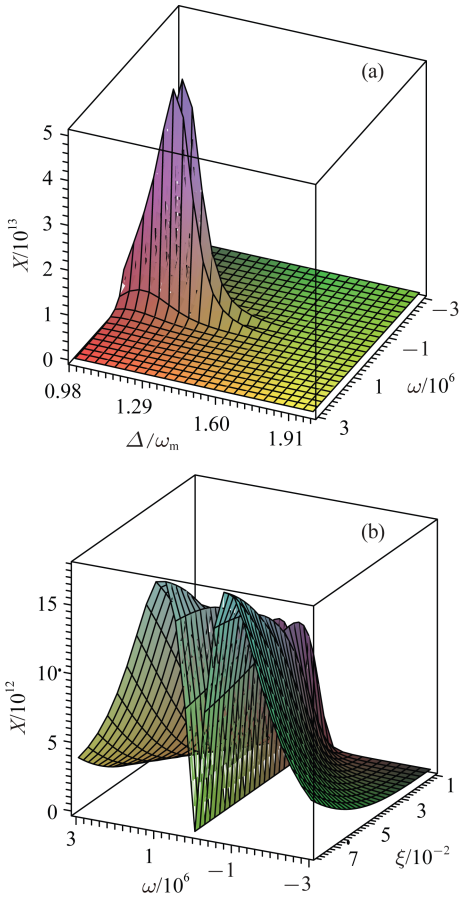


Fig. 2. (color online) Plot of the homodyne spectrum of the output fields $X(\omega)$ as the function of the normalized detuning $\Delta/\omega_{\rm m}$, ω, and ξ. The parameters are $\omega_{\rm m}=2\pi\times 51.8$ MHz, $\gamma_{\rm m}=8.2\pi\times 10^4$ Hz, $\theta=\pi/6$, $\kappa=30\pi$ MHz, $g=600$ Hz, $N=10$, $M=\sqrt{N(N+1)}$, $T=1$ K, $\Gamma=60\pi$ MHz for panel (a) $\xi=20$ mW and panel (b) $\Delta/\omega_{\rm m}=1$.

In Fig. 2, we give the plot of the homodyne spectrum of the output field with different parameters ω, ξ, and Δ. We can see that the homodyne spectrum of the output has the EIT dips. This finding suggests that the minimum of the homodyne spectrum of the output occurs at $\omega=0$. As $|\omega|$ increases, the homodyne spectrum of the output field is split into two maxima located symmetrically. Apparently, the parameters Δ/ω from 0.98 to 1.60 (Fig. 2(a)) and ξ from 10 mW to 70 mW (Fig. 2(b)) exhibit EIT dips, which stem from the destructive interference between the squeezed vacuum and the quantum field generated by the interaction between the coupling field and the movable mirrors. The width of the EIT dip is generally proportional to the power of the coupling field. From

Fig. 2(a), we find that with an increasing parameter ξ, the width of the EIT dips simultaneously decreases. Figure 2(b) shows that with the detuning Δ increasing, the width of the EIT dips gradually diminishes.

3. Generation of quadripartite macroscopic entanglement

To study quadripartite macroscopic entanglement in the proposed system, we calculate the fluctuations in the mirrors' amplitude. The parameter regime relevant to the generation of quadripartite optomechanical entanglement is a very large amplitude $c^{\rm s}$ with $|c^{\rm s}| \gg 1$ of the activity. In this case, we can derive the following linearized Langevin equations from Eq. (2):

$$\begin{aligned}
\delta\dot{Q}_1 &= \omega_{\rm m}\delta P_1,\\
\delta\dot{Q}_2 &= \omega_{\rm m}\delta P_2,\\
\delta\dot{Q}_3 &= \omega_{\rm m}\delta P_3,\\
\delta\dot{P}_1 &= g\cos^2(\theta/2)(\Re(c^{\rm s})\delta X+\Im(c^{\rm s})\delta Y)\\
&\quad -\omega_{\rm m}\delta Q_1-\gamma_{\rm m}\delta P_1+\xi_1,\\
\delta\dot{P}_2 &= -g\cos^2(\theta/2)(\Re(c^{\rm s})\delta X+\Im(c^{\rm s})\delta Y)\\
&\quad -\omega_{\rm m}\delta Q_2-\gamma_{\rm m}\delta P_2+\xi_2,\\
\delta\dot{P}_3 &= g\cos^2(\theta/2)(\Re(c^{\rm s})\delta X+\Im(c^{\rm s})\delta Y)\\
&\quad -\omega_{\rm m}\delta Q_3-\gamma_{\rm m}\delta P_3+\xi_3,\\
\delta\dot{X} &= -\kappa\delta X+\Delta\delta Y+\sqrt{2}\Im(c^{\rm s})(\delta Q_2-\delta Q_1\\
&\quad -\delta Q_3)+\sqrt{2\kappa}\delta X_{\rm in},\\
\delta\dot{Y} &= -\kappa\delta Y-\Delta\delta X-\sqrt{2}\Re(c^{\rm s})(\delta Q_2-\delta Q_1\\
&\quad -\delta Q_3)+\sqrt{2\kappa}\delta Y_{\rm in},
\end{aligned}\tag{10}$$

where the cavity field quadratures $\delta X=\delta c+\delta c^{\dagger}$ and $\delta Y=\mathrm{i}(\delta c^{\dagger}-\delta c)$ and the corresponding input noise quadratures $\delta X_{\rm in}=\delta c_{\rm in}+\delta c_{\rm in}^{\dagger}$ and $\delta Y_{\rm in}=\mathrm{i}(\delta c_{\rm in}^{\dagger}-\delta c_{\rm in})$ are defined. Equation (10) can then be rewritten in a matrix form as

$$\dot{\boldsymbol{f}}(t)=\boldsymbol{A}\boldsymbol{f}(t)+\boldsymbol{\chi}(t),\tag{11}$$

in which the transposes of the column vectors $\boldsymbol{f}(t)$ and $\boldsymbol{\chi}(t)$ can be expressed as $\boldsymbol{f}(t)^{\rm T}=(\delta Q_1,\delta P_1,\delta Q_2,\delta P_2,\delta Q_3,\delta P_3,\delta X,\delta Y)$ and $\boldsymbol{\chi}(t)^{\rm T}=(0,\xi_1,0,\ \xi_2,\ 0,\ \xi_3,\sqrt{2\kappa}\delta X_{\rm in},\sqrt{2\kappa}\delta Y_{\rm in})$, respectively. The drift matrix $\boldsymbol{A}$ for the above equation is given by

$$\boldsymbol{A}=\begin{pmatrix}
0 & \omega_{\rm m} & 0 & 0 & 0 & 0 & 0 & 0\\
-\omega_{\rm m} & -\gamma_{\rm m} & 0 & 0 & 0 & 0 & \eta_1 & \eta_2\\
0 & 0 & 0 & \omega_{\rm m} & 0 & 0 & 0 & 0\\
0 & 0 & -\omega_{\rm m} & -\gamma_{\rm m} & 0 & 0 & -\eta_1 & -\eta_2\\
0 & 0 & 0 & 0 & 0 & \omega_{\rm m} & 0 & 0\\
0 & 0 & 0 & 0 & -\omega_{\rm m} & -\gamma_{\rm m} & \eta_1 & \eta_2\\
-\eta_2 & 0 & \eta_2 & 0 & -\eta_2 & 0 & -\kappa & \Delta\\
\eta_1 & 0 & -\eta_1 & 0 & \eta_1 & 0 & -\Delta & -\kappa
\end{pmatrix},\tag{12}$$

with $\eta_1=g\cos^2(\theta/2)\Re(c^{\rm s})$, $\eta_2=g\cos^2(\theta/2)\Im(c^{\rm s})$. Our current objective is to study the entanglement properties in the steady state, which can be guaranteed to exist if the real parts of the eigenvalues of $\boldsymbol{A}$ are negative. The detailed conditions for this process to occur are derived via a simple stability-analysis test.[40] When the steady-state condition is satisfied, we can obtain the following equation for the stability correlation matrix:

$$\boldsymbol{A}\boldsymbol{V}+\boldsymbol{V}\boldsymbol{A}^{\rm T}=-\boldsymbol{D},\tag{13}$$

where $\boldsymbol{D}=\mathrm{Diag}[0,\gamma_{\rm m}(2n+1),0,\gamma_{\rm m}(2n+1),0,\gamma_{\rm m}(2n+1),\kappa,\kappa]$ with $n=(\exp\{\hbar\omega_{\rm m}/k_{\rm B}T\}-1)^{-1}$ is the average excitation number. The steady-state covariance matrix $\boldsymbol{V}$ of this system can be expressed as

$$\boldsymbol{V}=\begin{pmatrix}
\boldsymbol{K}_1 & \boldsymbol{L}_{12} & \boldsymbol{L}_{13} & \boldsymbol{L}_{1c}\\
\boldsymbol{L}_{12}^{\rm T} & \boldsymbol{K}_2 & \boldsymbol{L}_{23} & \boldsymbol{L}_{2c}\\
\boldsymbol{L}_{13}^{\rm T} & \boldsymbol{L}_{23}^{\rm T} & \boldsymbol{K}_3 & \boldsymbol{L}_{3c}\\
\boldsymbol{L}_{1c}^{\rm T} & \boldsymbol{L}_{2c}^{\rm T} & \boldsymbol{L}_{3c}^{\rm T} & \boldsymbol{K}_{\rm c}
\end{pmatrix},\tag{14}$$

in which $\boldsymbol{V}_{ij}=(\langle u_i(\infty)u_j(\infty)+\langle u_j(\infty)u_i(\infty)\rangle)/2$, with $\boldsymbol{u}^{\rm T}(\infty)=(\delta Q_j(\infty),\delta P_j(\infty),X(\infty),\delta Y(\infty))$ is the vector of the fluctuation operators at the steady state ($t\longrightarrow\infty$). In Eq. (14), $\boldsymbol{K}_j$ is a 2×2 matrix describing the local properties of mode j ($j=1,2,3,c$), whereas the $\boldsymbol{L}_{ij}$ ($i,j=1,2,3$) matrix indicates intermode correlations. To investigate the behavior of the entanglement among the elements of the quadripartite system, we employ logarithmic negativity E_N[41–43] to judge entanglement. In the continuous variable case, E_N can be defined as[43]

$$E_N=\max[0,-\log_2\nu_-],\tag{15}$$

where the smallest eigenvalue

$$\nu_-=\sqrt{\frac{\Delta(\boldsymbol{\Gamma})-\sqrt{\Delta(\boldsymbol{\Gamma})^2-4\mathrm{Det}\boldsymbol{\Gamma}}}{2}},$$

with $\Delta(\Gamma)=\det\boldsymbol{A}+\det\boldsymbol{B}-2\det\boldsymbol{C}$, and the 2×2 block form of the correlation matrix $\boldsymbol{\Gamma}$ as

$$\Gamma=\begin{pmatrix}\boldsymbol{A} & \boldsymbol{C}\\ \boldsymbol{C}^{\rm T} & \boldsymbol{B}\end{pmatrix}.\tag{16}$$

The element of the covariance matrix Γ_{ij} is derived from the 4×4 matrix from $\boldsymbol{V}$ by taking the block matrix in Eq. (14). We will describe and quantify the bipartite $\boldsymbol{C}$–$\boldsymbol{V}$ entanglement in both the cavity field–mirror and mirror–to–mirror subsystems. In our numerical calculations, we take the systems? parameters: $\xi=20$ mW, $\omega_{\rm m}=9.5\times10^8$ Hz, $\gamma_{\rm m}=100$ Hz, $\theta=\pi/6$, $\kappa=6.8$ MHz, $g=200$ Hz, and $T=8$ mK, which are based on the current experiments? conditions.[44–46] We numerically investigate the entanglement in the cavity field–mirrors subsystem.

First, we numerically investigate the entanglement in the cavity field–mirror subsystem. According to the numerical calculations, we find that the logarithmic negativity E_N of

three field–mirror subsystems are equal in value. This finding can be verified from the second term of Eq. (1), where the three mirrors are symmetrical. Thus, the entanglement of all field–mirror subsystems has the same value.

In Fig. 3(a), the logarithmic negativity E_N of the field–mirror subsystem is plotted with parameter Δ. The curve implies a strong C–V entanglement between field–mirror subsystems. That is, C–V entanglement persists between the field and any of the three movable mirrors when parameter Δ ranges from 0.7 to 1.2. We can clearly see that the value E_N is close to its minimum when $\Delta = \omega_{\rm m}$. For the far detuning cavity, the input power can be reduced, which will set the system into a condition of small backaction. The robustness of this entanglement with respect to environmental temperature is shown in Fig. 3(b). The relevant result is that the entanglement of a field–mirror subsystem persists for temperatures above 9 mK.

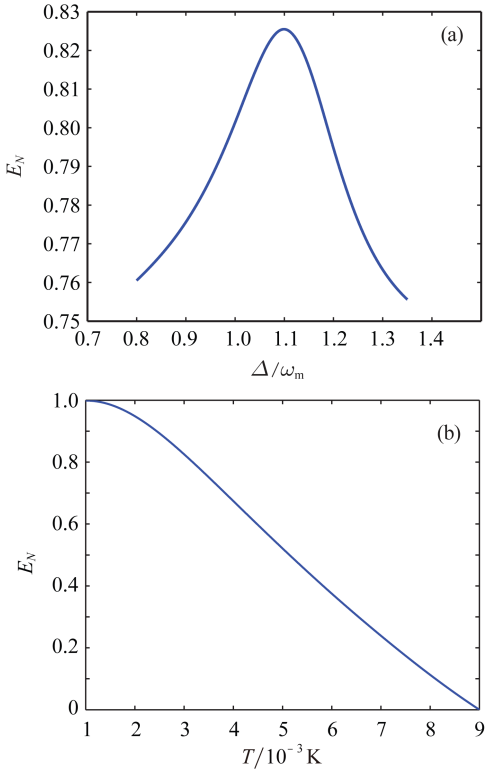


Fig. 3. (color online) Plot of the steady-state entanglement described by the logarithmic negativity E_N as a function of the normalized detuning $\Delta/\omega_{\rm m}$. The parameters are $\xi = 50$ mW, $\omega_{\rm m} = 9.5 \times 10^8$ Hz, $\gamma_{\rm m} = 100$ Hz, $\theta = \pi/3$, $\kappa = 6.8$ MHz, $g = 200$ Hz, (a) $T = 2$ mK and (b) $\Delta/\omega = 1$.

Moreover, we also calculated the C–V entanglement among the mirror–to–mirror subsystems of the three movable mirrors M_1, M_2, and M_3. On the basis of the calculation results, the logarithmic negativity E_N of any mirror–to–mirror subsystem is close to 0.99 using the same parameters as with the previous model. That is, strong C–V entanglement exists among the mirror–to–mirror subsystems. According to the model or the Hamiltonian of this system, although the three mirrors never interact directly, the cavity field acts as a bus for the cross talk of the three mirrors. That is, any entanglement among the mirror–to–mirror subsystems is an indication of a coherent field–mirror interaction induced by the cavity field. The corresponding quadripartite state violates the positivity of the partial transposition criterion with respect to all partitions, indicating that the state is not biseparable with respect to any split and reflecting multipartite entanglement in this sense.[19] Hence, we arrive at a very important result, that is, genuine quadripartite C–V entanglement can be obtained among the subsystems.

Finally, we will discuss how to use logarithmic negativity to ascertain entanglement. In this system, the quadripartite state violates the positivity of the partial transposition criterion with respect to all partitions, which means that the state is not biseparable with respect to any split and reflecting multipartite entanglement in this aspect.[19] Obviously, this process can exclude biseparability for any split, but one possibility is that a convex combination of biseparable states remains with respect to different subsystems. To take an extreme example, an entangled state exists between two parties only, whereas the specific modes that share this entanglement are unknown. Nevertheless, the optomechanical state has been verified to be a genuinely multipartite entanglement in the stronger sense, using the optimal entanglement witnesses for Gaussian states.[19] Hence, genuine quadripartite entanglement exists among the subsystems.

4. Discussion and conclusions

A ring cavity with one fixed mirror and three movable perfectly reflecting mirrors is investigated. Using a linearized fluctuation analysis, we derived the quantum fluctuations and stability correlation matrix of this system. The mean square fluctuations in position and momentum of the cavity field and the movable mirrors are presented. We have discussed EIT using quantum fields in optomechanical systems under a wide range of parameter conditions. The results show that the homodyne spectrum of the output has perfect EIT dips and that the width of the EIT dips can be controlled by the parameters ξ and Δ.

We have also discussed the entanglement among field–mirror subsystems, as well as that among mirror–to–mirror subsystems, in a quadripartite system. Numerical results show that genuine quadripartite macroscopic entanglement can be generated despite the lack of direct interaction among the movable mirrors. This condition facilitates the generation of C–V entanglement among the macroscopic objects, reminding us of the utility of such an entanglement as an effective treatment regimen for the indirect manipulation of the mirror state through cavity–field control.

References

[1] Nielson M A and Chuang I L 2000 *Quantum Computation and Quantum Information* (Cambridge: Cambridge University Press)
[2] Horodecki R, Horodecki P, Horodecki M and Horodecki K 2009 *Rev. Mod. Phys.* **81** 865
[3] Huang S and Agarwal G S 2011 *Phys. Rev.* A **83** 043826
[4] Rocheleau T, Ndukum T, Macklin C, Hertzberg J B, Clerk A A and Schwab K C 2010 *Nature* **463** 72
[5] O'Connell A D, Hofheinz M and Ansmann M 2010 *Nature* **464** 697
[6] Brown K R, Ospelkaus C, Colombe Y, Wilson A C and Leibfried D 2011 *Nature* **471** 196
[7] Liao J Q and Law C K 2011 *Phys. Rev.* A **83** 033820
[8] Khalili F, Danilishin S, Miao H, Müller-Ebhardt H, Yang H and Chen Y 2010 *Phys. Rev. Lett.* **105** 070403
[9] Miao H, Zhao C, Ju L and Blair D G 2009 *Phys. Rev.* A **79** 063801
[10] Zhao C, Ju L, Miao H, Gras S, Fan Y and Blair D G 2009 *Phys. Rev. Lett.* **102** 243902
[11] Mi X W, Bai J X and Li D J 2012 *Chin. Phys.* B **21** 030303
[12] Zou H L, Xu J X and Jiang J 2008 *Chin. Phys.* B **17** 117
[13] Vitali D, Gigan S, Ferreira A, Böhm H R, Tombesi P, Guerreiro A, Vedral V, Zeilinger A and Aspelmeyer M 2007 *Phys. Rev. Lett.* **98** 030405
[14] Genes C, Mari A, Tombesi P and Vitali D 2008 *Phys. Rev.* A **78** 032316
[15] Mancini S, Giovannetti V, Vitali D and Tombesi P 2002 *Phys. Rev. Lett.* **88** 120401
[16] Zhang J, Peng K and Braunstein S L 2003 *Phys. Rev.* A **68** 013808
[17] Pinard M, Dantan A, Vitali D, Arcizet O, Briant T and Heidmann A 2005 *Europhys. Lett.* **72** 747
[18] Huang S M and Agarwal G S 2009 *New J. Phys.* **11** 103044
[19] Paternostro M, Vitali D, Gigan S, Kim M S, Brukner C, Eisert J and Aspelmeyer M 2007 *Phys. Rev. Lett.* **99** 250401
[20] Ian H, Liu Y X and Nori F 2010 *Phys. Rev.* A **81** 063823
[21] Roghani M, Breuer H B and Helm H 2010 *Phys. Rev.* A **81** 033418
[22] Li Z H, Li Y, Dou Y F and Zhang J X 2012 *Chin. Phys.* B **21** 034204
[23] Lee Y C, Tsai C C, Chang Y Y, Huang C H and Chui H C 2011 *Chin. Phys.* B **20** 073101
[24] Niu J Y, Pei L Y, Wu L A and Fu P M 2010 *Chin. Phys.* B **19** 113209
[25] Luo B, Hang C, Li H J and Huang G X 2010 *Chin. Phys.* B **19** 054214
[26] Weis S, Riviére R, Deléglise S, Gavartin E, Arcizet O, Schliesser A and Kippenberg T J 2010 *Science* **330** 1520
[27] Eisaman M D, André A, Massou F, Fleischhauer M and Zibrov A S 2005 *Nature* **438** 837
[28] Appel J, Figueroa E, Korystov D, Lobino M and Lvovsky A I 2008 *Phys. Rev. Lett.* **100** 093602
[29] Lobino M, Kupchak C, Figueroa E and Lvovsky A I 2009 *Phys. Rev. Lett.* **102** 203601
[30] Kocharovskaya O, Rostovtsev Y and Scully M O 2001 *Phys. Rev. Lett.* **86** 628
[31] Han Y, Cheng J and Zhou L 2011 *J. Phys.* B: *At. Mol. Opt. Phys.* **44** 165505
[32] Agarwal G S and Huang S 2010 *Phys. Rev.* A **81** 041803
[33] Weis S, Riviére R, Deléglise S and Gavartin E 2010 *Science* **300** 1520
[34] Lin Q, Rosenberg J, Chang D and Camachom R 2010 *Nat. Photon.* **4** 236
[35] Safavi-Naeini A H, Mayer Alegre T P, Chan J and Eichenfield M 2011 *Nature* **472** 69
[36] Gröblacher S, Hammerer K, Vanner M R and Aspelmeyer M 2009 *Nature* **460** 724
[37] Gorodetsky M L, Schliesser A, Anetsberger G, Deleglise S and Kippenberg T J 2010 *Opt. Express* **18** 23236
[38] Gardiner C W and Zoller P 1991 *Quantum Noise* (Berlin: Springer-Verlag)
[39] Giovannetti V and Vitali D 2001 *Phys. Rev.* A **63** 023812
[40] DeJesus E X and Kaufman C 1987 *Phys. Rev.* A **35** 5288
[41] Laurat J, Keller G and Oliveira-Huguenin J A 2005 *J. Opt.* B: *Quantum Semiclass. Opt.* **7** S577
[42] Vidal G and Werner R F 2002 *Phys. Rev.* A **65** 032314
[43] Adesso G, Serafini A and Illuminati F 2004 *Phys. Rev.* A **70** 022318
[44] Gigan S, Böhm H R, Paternostro M and Blaser F 2006 *Nature* **444** 67
[45] Kleckner D and Bouwmeester D 2006 *Nature* **444** 75
[46] Marquardt F, Chen J P, Clerk A A and Girvin S M 2007 *Phys. Rev. Lett.* **99** 093902